

Pharmacoproteomics of 4-Phenylbutyrate-Treated IB3-1 Cystic Fibrosis Bronchial Epithelial Cells

Om V. Singh,[†] Neeraj Vij,[†] Peter J. Mogayzel, Jr.,[†] Cathy Jozwik,[‡] Harvey B. Pollard,[‡] and Pamela L. Zeitlin^{*,†}

Department of Pediatrics, The Johns Hopkins School of Medicine, Baltimore, Maryland 21209, and Department of Anatomy, Physiology and Genetics, Uniformed Services University School of Medicine, Bethesda, Maryland 20814

Received September 21, 2005

4-Phenylbutyrate (4-PBA) is an oral butyrate derivative that has recently been approved for treatment of urea cycle disorders and is under investigation in clinical trials of cancer, hemoglobinopathies, and cystic fibrosis (CF). We hypothesized that proteome profiling of IB3-1 cystic fibrosis bronchial epithelial cells treated with 4-PBA would identify butyrate-responsive cellular chaperones, protein processing enzymes, and cell trafficking molecules associated with the amelioration of the chloride transport defect in these cells. Protein profiles were analyzed by two-dimensional gel electrophoresis and mass spectrometry. Over a *pI* range of 4–7 and molecular weight from 20 to 150 kDa a total of 85 differentially expressed proteins were detected. Most of the identified proteins were chaperones, catalytic enzymes, and proteins comprising structural elements, cellular defense, protein biosynthesis, trafficking activity, and ion transport. Subsets of these proteins were confirmed by immunoblot analysis. These data represent a first-draft of the pharmacoproteomics map of 4-PBA treated cystic fibrosis bronchial epithelial cells.

Keywords: cystic fibrosis • chaperone • chloride transport • proteasome • two-dimensional gel electrophoresis

Introduction

Cystic Fibrosis (CF), one of the most common life-shortening autosomal recessive inherited diseases, results from mutations in the cystic fibrosis transmembrane conductance regulator (CFTR) gene.¹ The CFTR protein forms an ion channel permeable to Cl⁻ and other large anions.² The most common mutation worldwide is a three-base-pair deletion that results in the loss of phenylalanine at position 508 (Δ F508) of CFTR.^{3,4} This mutation leads to abnormal processing in the endoplasmic reticulum. Most of the newly synthesized mutant CFTR is retained in the endoplasmic reticulum (ER) and targeted for degradation by ubiquitination and proteolysis.^{5,6} Limited amounts of Δ F508–CFTR may escape from the ER under certain favorable conditions (such as 27°C, 10% glycerol, or $\geq 100 \mu$ M 4-PBA) and traffic to the plasma membrane, where the rescued mutant CFTR channels function with a reduced open time.^{7–9} The clinical spectrum of CF symptoms suggests that increasing the amount of CFTR at the cell surface might improve clinical outcome. We and others have shown that Δ F508–CFTR can be increased in the plasma membrane with nontoxic doses of sodium 4-phenylbutyrate (4-PBA); SERCA calcium pump inhibitors; compounds from the family of

benzo[c]quinolizinium molecules; and chemical chaperones such as glycerol, xanthenes, or growth at reduced temperature.^{9–12}

Short chain fatty acid derivatives of butyric acid, including 4-PBA, promote Δ F508 CFTR trafficking by mechanisms that are distinct from those attributed to the chemical chaperones.^{13,14} However, while the molecular mechanisms by which 4-PBA mediates its effects are still not well understood, regulation of histone hyperacetylation, DNA methylation and high-mobility group modification have been reviewed by Monneret.¹⁵ Butyrates are also known to affect genes involved in cell cycle regulation, including p16, c-myc, p21^{WAF} and cyclooxygenase.^{16–18}

In our present study we utilize the IB3-1 CF bronchial epithelial cell line that we have previously shown responds to low concentrations of 4-PBA with an increase in mature Δ F508–CFTR.^{10,14} Moreover, during phase I and phase II clinical trials of 4-PBA in CF patients, we observed partial restoration of CFTR-chloride channel function in nasal epithelia.¹⁹

In a recent study, we used Affymetrix technology to examine the genomics of 4-PBA in CF cells.²⁰ We found that changes in gene expression of cellular chaperones, including upregulation of HSP70, were observed in association with the rescue of mutant CFTR. However, parallels between mRNA production and cognate protein responses are infrequent in eukaryotic cells.²¹ Therefore, to test the genomic conclusions at the protein expression level, we have adopted a global pharmacoproteomic approach. On the basis of the earlier pharmacogenomics data,

* To whom correspondence should be addressed. Pamela L. Zeitlin, Professor of Pediatrics, Park 316, 600 N. Wolfe St, Baltimore, MD 21287. Tel: (410) 614-5637. Fax: (410) 955-1030. E-mail: pzeitlin@jhmi.edu.

[†] The Johns Hopkins School of Medicine.

[‡] Uniformed Services University School of Medicine.

we hypothesized that 4-PBA might affect not only cellular chaperones such as HSP70 and HSC70, but also other related protein processing enzymes and cell trafficking molecules. We anticipated that other informative proteins beyond the subset of 4-PBA-affected genes detectable at the mRNA level would be discovered by this approach.

In this paper, we report that a proteomic signature for 4-PBA action can be identified, and that a subset of these proteins correlates with pharmacogenomic predictions.²⁰ Importantly, the pharmacoproteomic analysis identifies additional proteins that were not detectable with the purely genomic approach. In addition, by combining our earlier genomics data with this new pharmacoproteomics data, we can gain further insight into the systemic effects of 4-PBA.

Materials and Methods

Cell Culture. IB3-1 cells (Δ F508/W1282X CF bronchial epithelial cells)²² were grown on uncoated 75 cm² tissue culture flasks (Falcon, Franklin Lakes, NJ) in a 5% CO₂ incubator at 37 °C for 48–72 h to reach 80% confluency. The standard growth medium was gentamicin-free LHC-8 (Biofluids, Rockville, MD) supplemented with 5% fetal bovine serum (Biofluids), 100 U/mL of penicillin-streptomycin (GIBCO BRL, Gaithersburg, MD), 80 μ g/mL of tobramycin (Eli Lilly, Indianapolis, IN) and 2.5 μ g/mL of Fungizone (Biofluids). During the course of our experiments, potential problems caused by clonal drift were avoided by using new batches of frozen cells after every 12 passages. Unless otherwise stated, 5 mM sodium 4-phenylbutyrate (4-PBA, Medicis Pharmaceuticals, Scottsdale, AZ) was added for 48 h and pH was maintained at 7.4.

Sample Preparation for Two-Dimensional Gel Electrophoresis. The IB3-1 cells were harvested after 48 h of 4-PBA treatment, rinsed twice with ice cold 1 \times PBS, pH 7.4 (GIBCO), and lysed with 2-D lysis buffer (8 M Urea; 4% CHAPS; 20 mM Tris-HCL pH 8.8) containing freshly added inhibitors 2 mM phenylmethylsulfonyl fluoride, 0.2 U/mL aprotinin, and 10 μ M sodium orthovanadate followed by incubation on ice for 30 min. The cell lysate was collected and loaded on QIAshredder (Qiagen), centrifuged at 15 000 \times *g* at 4 °C for 5 min, the flow through was collected and protein concentration was quantified using RCDL protein assay kit (Bio-Rad, Hercules, CA) with BSA as a standard. The protein samples were aliquoted and stored at –80 °C.

Two-Dimensional Gel Electrophoresis (2-DE). 2-DE was performed as previously described with modifications.²³ Briefly, the total cellular protein extracts were separated by first-dimensional isoelectric focusing (IEF) using pre-cast dry 17 cm immobilized pH Gradient (IPG) strips (Bio-Rad) on a IPGphor unit (Bio-Rad). Each IPG strip was re-hydrated for 12 h with 100 μ g total protein in 300 μ L of IEF rehydration buffer (7 M Urea; 2 M Thiourea; 4% CHAPS; 0.5% Carrier ampholyte; 40 mM Dithiothreitol (DTT); 0.002% Bromophenol Blue). IEF was carried out using the following conditions: (i) 250 V for 20 min on linear ramp, (ii) 10 000 V for 2 h on linear ramp, (iii) 10 000 V at 45 000 V-hr on rapid ramp, (iv) hold at 500 V on rapid ramp until IPG strips were removed from first dimension. The strips were then subjected to a 2-step equilibration using equilibration buffer I (6 M Urea; 2% SDS; 0.375 M Tris-HCL pH 8.8; 20% Glycerol and 130 mM DTT) followed by equilibration buffer II (6 M Urea; 2% SDS; 0.375 M Tris-HCL pH 8.8; 20% Glycerol and 135 mM Iodoacetamide) for 15 min each just before proceeding for 2-DE. The second dimensional electrophoresis was performed on 1.0 mm 10% SDS-PAGE gels at 50 V for 30 min followed by 100 W until the blue dye front arrives

at the bottom of the gel using an Amersham Pharmacia Iso-DALT electrophoresis unit.

Image Acquisition and 2-D Gel Spot Pattern Analysis. Any two gels undergoing direct comparison were always run and silver stained in parallel. Silver staining was performed using the MS-compatible SilverQuest Silver staining kit (Invitrogen, Carlsbad, CA). Stained gel images were acquired using Molecular Imager FX (Bio-Rad). Consistent replicate images were further processed for spot detection, gel alignment and spot quantification by match ratio using Progenesis Nonlinear Dynamics software version 2005. Quantitative variations in proteins are expressed as volumes of spots with reference to a constant spot in each experiment. To compensate for variations in gel staining and differences in protein spot numbers for each gel, normalized spot volumes were used for comparison of protein expression levels. The normalized spot volume was automatically calculated by the software as the single spot volume divided by the total spot volume and then multiplied by the total spot area.

Enzymatic Digestion of Protein Spots. Selected silver-stained protein spots were excised manually with a plastic plunger (The gel, San Francisco, CA) and transferred to, an acetonitrile (ACN) pre-rinsed (500 μ L), eppendorf tube. In addition to these protein spots, 15 blank spots were excised from the gel as controls. Prior to peptide digestion, the protein gel pieces were destained by adding a 1:1 mix of 30 mM potassium ferrocyanide and 100 mM sodium thiosulfate until gel pieces lost the brown color, followed by three washes with 200 μ L proteomics grade water (Bio-Rad). Destained gel pieces were washed with 20 mM NH₄HCO₃ and dehydrated with ACN, twice for 10 min each. Finally, the dried gel pieces were swelled in 20 μ L (10 ng/ μ L) sequencing-grade modified trypsin (Promega, Madison, WI) in 20 mM NH₄HCO₃, pH 8.5 (Sigma, St. Louis, MO) and incubated on ice for 45 min. Excess trypsin was removed around the gel pieces and replaced with 10 mM NH₄HCO₃, pH 8.5. Protein digestion was continued by incubating gel pieces at 37 °C overnight with gentle shaking. Peptides were extracted from gel pieces by adding 200 μ L of 0.1% trifluoroacetic acid (TFA) in 60% ACN followed by vigorous shaking for 60 min at 30 °C. Supernatant was collected and dried in a speed vac concentrator (Eppendorf) and resulting peptides were solubilized in 5 μ L 0.1% TFA.

Peptide Mass Fingerprinting by Mass Spectrometry. The extracted peptide mixture was desalted with an in-tip reversed phase column (C18 Zip-Tip; Millipore).²⁴ The peptide mixture was eluted from the Zip-Tip with 2 μ L of matrix solution (10 mg/mL α -cyano-4-hydroxycinnamic acid (Sigma) in 60% ACN/ 0.1% TFA) and directly spotted onto a matrix assisted laser desorption ionization (MALDI) target plate. Mass analyses were performed using a matrix assisted laser desorption ionization-time-of-flight (MALDI-TOF) mass spectrometer (Voyager DE-STR, Applied Biosystems, Framingham, MA) equipped with a 337 nm nitrogen laser. Samples were analyzed in reflectron mode by TOF at an accelerating potential 20 kV. The average of 3 scans (each containing 75 spectra) that passed the accepted criterion of peak intensity were automatically selected and saved. Mass spectra's were automatically calibrated upon acquisition using two point residual porcine trypsin autolytic fragments (842.51 and 2210.10 [M⁺H⁺] ions) and matrix added standard bradykinin and ACTH peaks (757.39 and 2,465.19 [M⁺H⁺] ions) from Sigma.

Identification of Proteins. The individual proteins were identified by searching in the NCBI nonredundant databases

using ProFound-peptide Mapping (The Rockefeller University Edition, Version 4.10.5). All mass searches were performed using the short form of ProFound-peptide mapping under *Homo sapiens* taxonomic category for only single protein under pre-assumed experimental mass and *pI* range. The search parameters were allowed complete modification with Iodoacetamide (Cys). The criteria for positive identification of proteins were set as follows: (i) the MS match for at least 4 peptides; (ii) 20–50 ppm or better mass accuracy; (iii) the matched peptides covered at least 15% of the whole protein sequence with a significant Z score (> 90% probability); (iv) comparable *pI* and molecular weight obtained from experimental image analysis.

Protein Information. Information about identified proteins and putative functions was found on Swiss-Prot database at the ExPASy Molecular Biology Server (www.expasy.org).

Immunoblot Analysis of 4-PBA Modulated Proteins. Control and 4-PBA-treated IB3-1 cells were cultured for 48 h and the immunoblot analysis of the protein samples was performed as described earlier.¹⁰ CFTR band B and C were recognized by primary antisera (1:1000), generated in rabbit against the 181 peptide from CFTR NBD domain.²⁵ Other primary antibodies used were mouse monoclonal for HSP70 (1:1000) and HOP (1:1000) (StressGene Biotechnologies, Victoria, BC), goat polyclonal for GRP78 (1:500), TCP1 (1:1000) and β -actin (1:1000), mouse monoclonal for Cytokeratin 18 (1:1000) (Santa Cruz Biotechnology, Inc.), and rabbit polyclonal for Proteasome 26S non-ATPase subunit 11 (1:1000) (Orbigen Inc.) and ARP2 or ATRC2 (1:1000) (Chemicon International). Secondary antibodies used were donkey anti-rabbit IgG-horseradish peroxidase conjugate and sheep anti-mouse IgG-horseradish peroxidase conjugate (Amersham, Arlington Heights, IL), and rabbit anti-goat IgG-peroxidase conjugate (Sigma, St. Louis MO). Non-specific binding was eliminated by pre-blocking the nitrocellulose membrane with 5% nonfat dry milk in PBS-0.05% Tween 20 for 1 h.

Densitometric Analysis. Fluorographic images were digitized into eight-bit tagged image format files using scan jet Plus (Hawlett-Packard). Baseline density of the area surrounding the bands was determined by two-dimensional integration with Quantity One image analysis software (Bio-Rad) and local background was subtracted. Densitometric analysis was performed using the percent volume ratio of selected bands, i.e., total signal intensity inside a defined boundary drawn on an image. One-way ANOVAs followed by least significant differences (Tukey's Honestly Significant Difference) were performed on the gel bands determined from between control and 4-PBA treated. A *P* value <0.05 was considered to have statistical significance.

Results

4-PBA Mediated Correction of $\Delta F508$ CFTR in IB3-1 Cells.

We studied the immortalized CF bronchial epithelial cell line IB3-1,²² (CFTR genotype $\Delta F508/W1282X$). IB3-1 expresses the $\Delta F508$ CFTR protein only, because the W1282X mutation produces an unstable, and therefore untranslated, mRNA.^{26,27} We have previously published the dose response curve for 4-PBA mediated rescue of $\Delta F508$ CFTR processing in IB3-1 cells. A dose of 5 mM 4-PBA for 48 h produces the most efficient rescue of CFTR from degradation.¹⁰ As shown in Figure 1, when IB3-1 cells were exposed to 5 mM 4-PBA at 37 °C for 48 h and analyzed by immunoblotting with anti-CFTR 181 antibody, immature mutant protein was processed to the higher molec-

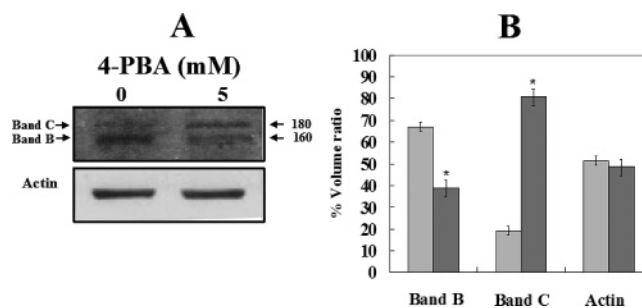


Figure 1. Maturation of CFTR from band B to band C by 4-PBA. A: IB3-1 cells were incubated with 5 mM 4-PBA for 48 h. Protein lysates were prepared as described in Materials and Methods. Total protein (35 μ g) was resolved on a 9% SDS-PAGE. Proteins were electrophoretically transferred to nitrocellulose, and immunodetection of CFTR was performed using primary antisera CFTR 181. Band B and C, position of immature and mature CFTR, respectively, molecular mass in kDa. B: Densitometry was performed as described in Materials and Methods. Light bars represent control band B and band C in untreated condition and solid bars represents band B and band C after 4-PBA treatment. Values are mean \pm SEM of density of gel bands determined from between control ($n = 3$) and 4-PBA treated ($n = 3$) (* $P < 0.05$).

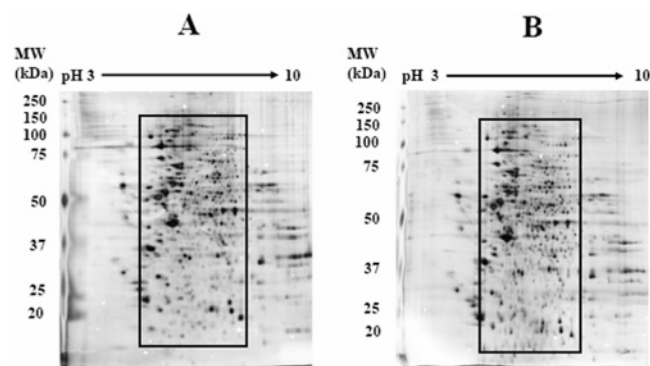


Figure 2. 2-DE map image of proteins identified by silver staining in IB3-1 cells. Whole cell lysates were processed as described in the Materials and Methods. Proteins (100 μ g) were loaded onto an IPG strip (pH 3–10) and subsequently separated by mass on a 10% SDS-PAGE gel. The gel was stained with MS compatible silver stain and the filtered images were generated by Progenesis Nonlinear Dynamic software (version 2005). Images obtained were reproducible in six independent gels from three different experiments. (A) IB3-1 cells, untreated; (B) IB3-1 cells, 5 mM 4-PBA, 48 h. The rectangles delineate the regions containing proteins that are differentially expressed on 4-PBA treatment.

ular weight form. Untreated IB3-1 cells expressed predominantly band B (160 kDa, Figure 1A). Treatment with 5 mM 4-PBA for 48 h led to enhanced processing of band B to band C (180 kDa, Figure 1B). The relative intensities of CFTR band B and band C were quantified by densitometry and this analysis confirmed the predominance of band C after treatment with 5 mM 4-PBA (Figure 1B).

2-DE Protein Profile of 4-PBA-Treated IB3-1 Cells. Preliminary screening of proteins differentially expressed by 1 and 5 mM 4-PBA suggested better detection of differentially expressed protein with the higher dose. Therefore, 5 mM 4-PBA was chosen for further studies. As shown in Figure 2, over 1000 proteins were captured in the pH range of 3–10 and in the molecular weight range of 20–250 kDa. Software analysis of

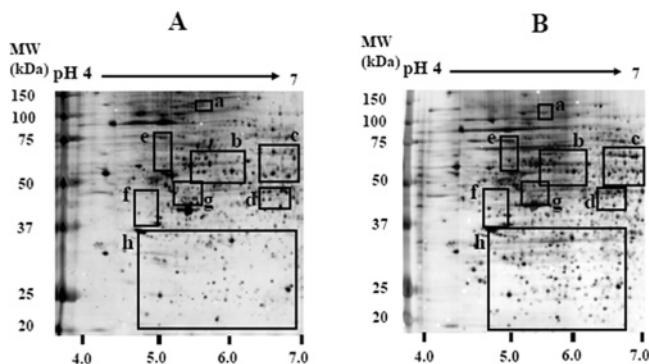


Figure 3. 2-DE image of pH range 4–7 of IB3-1 cells treated with 4-PBA. The whole cell lysates were prepared as described in Materials and Methods. Proteins (100 μ g) underwent isoelectric focusing onto an IPG strip (pH 4–7 NL) and separation by mass on a 10% SDS-PAGE gel. The MS compatible silver stained gels were scanned, and filtered images were generated for the analysis of differential expression of protein spots using Progenesis Nonlinear Dynamic software (version 2005). (A) IB3-1 cells, untreated; (B) IB3-1 cells, 5 mM 4-PBA, 48 h. Selected rectangles delineate the regions containing proteins that are differentially expressed on 4-PBA treatment. The patterns of protein spots on 2-DE gels were highly reproducible with and without 4-PBA treatment in six independent gels from three different experiments.

these images confirmed that the best resolution of the spots occurred for proteins focused between pH 4 and 7. Furthermore, by focusing between pH 4 to 7, the protein profiles in this narrower pH range resolved over 3000 protein spots (Figure 3).

High Resolution 2-DE Protein Profile of 4-PBA-Treated IB3-1 Cells. To emphasize large scale changes, we selected protein images after normalization that were greater than 2-fold in magnitude as detected by silver staining. Eight different regions on two typical 2-DE profiles between pH 4 to 7 are highlighted in Figure 4a-h. Out of eighty-five differentially expressed proteins, 64 proteins increased and 21 proteins decreased with 4-PBA treatment. As depicted in Figure 4a-h, the intensities of protein spots were clearly increased or decreased after 4-PBA treatment. Overall values of the spots based on gel-estimated M_r and pI , matched well with the corresponding to theoretical values with the exception of alanyl-tRNA synthetase (spot no. 2, Figure 4a; Table 1). For more than 95% of the spots, a sequence coverage exceeding 15% has been obtained. In the present study, the majority of the proteins were identified based on five or more matching peptides. The spot pattern was highly reproducible in six independent gels from three different experiments. The most prominent protein Actin- β (MW 42 kDa, pI 5.2) was selected as a reference protein spot for the orientation of 2-D gels as detected earlier.²⁸

Functional Characterization of 4-PBA Modulated Proteins. Among 85 differentially expressed proteins, 43 protein spots were identified and sorted according to functional category (Table 1). Out of the 30 cellular communication, metabolism and signal transduction proteins, 12 proteins involved in protein synthesis and processing were found to be upregulated. Of these 12 proteins, spot no. 18 (HSP70; Figure 4c) is well-known to have an impact on CFTR trafficking^{10,29–32} and was more than 4-fold increased after 4-PBA treatment. Among the more than 4-fold upregulated proteins, protein spot no. 21

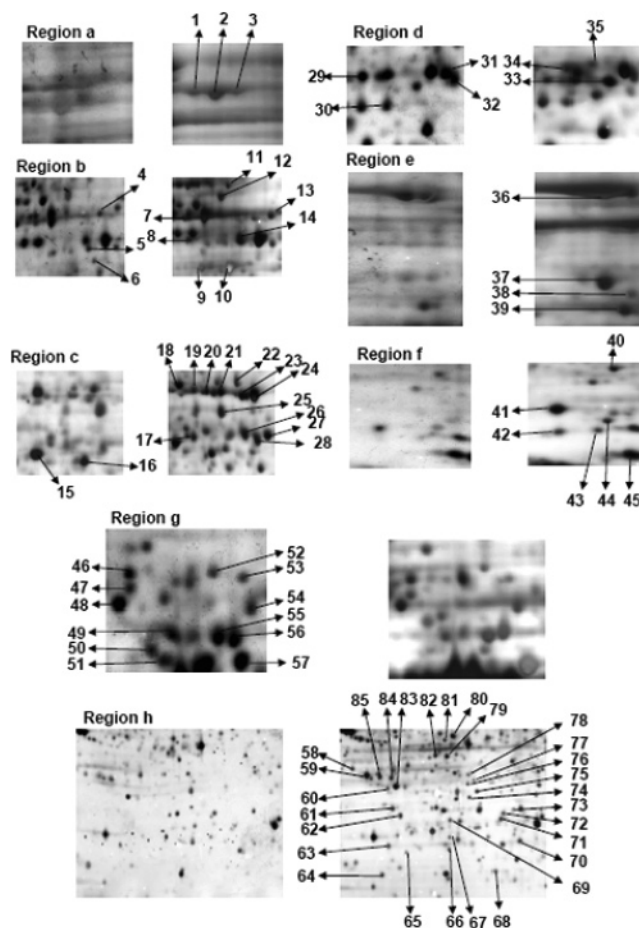


Figure 4. 2-DE analysis of 8 informative regions from the gels in Figure 3. The 8 regions have been magnified and arrows added to label the differentially expressed proteins. Left and right panel of each region contain proteins from control and 5 mM 4-PBA treated IB3-1 cells, respectively. The corresponding locations on the gels were excised, trypsinized and analyzed by MALDI-TOF-MS as described in the Materials and Methods. The proteins were subsequently identified by tryptic peptide mass fingerprints. Table 1 contains a list of the identified protein spots.

(Figure 4c) was identified as HSP70/HSP90 organizing protein (HoP) that has been found related with the assembly of the HSP70/HSP90 chaperone heterocomplex.^{33,34} Another upregulated protein GRP78 (HSPA5) (Figure 4e, spot no. 36), also referred to as ‘immunoglobulin heavy chain-binding protein’ (BiP), is also a member of the heat shock protein-70 (HSP70) family, and is potentially involved in the folding and assembly of proteins in the ER. Interestingly, T-complex proteins 1 (TCP-1; spot no. 13; Figure 4b) and chaperonin containing TCP1 subunit 6A (CCT; spot no. 25; Figure 4c), known to mediate protein folding in the eukaryotic cytosol, were also upregulated.

The proteasome family of proteins was also modulated by 4-PBA. The expression of proteasome (prosome, macropain) 26S subunit, non-ATPase (spot no. 32; Figure 4d) was decreased with butyrate treatment. The proteasome plays a central role in the proteolysis of ubiquitinated cellular proteins. Interestingly, some of the members of the translation initiation factor family, eukaryotic translation initiation factor 3 and 4a, were also downregulated after 4-PBA treatment (spot no. 50 and 56; Figure 4g), indicating that 4-PBA regulates proteins involved in biosynthesis and degradation.

Table 1. List of Differentially Expressed Identified Protein Spots with In-Gel Digestion and MALDI-TOF MS Analysis Regulated by 4-PBA Treatment in IB3-1 Cells

Locus Link ID	HUGO ^a name	protein description	ext'd Z score ^b	theor. M _r (kDa)/pI	exper. M _r (kDa)/pI	matches (n)	coverage (%)	4-PBA regulation	spot no.
Cellular Communication and Signal Transduction									
Protein Synthesis, Processing and Protein Fate									
NP_001596	AARS	Alanyl-tRNA synthetase	2.34	107.53/5.3	130/5.6	14	27	↑	2
P17987	TCP1	T-complex protein 1, alpha subunit (TCP-1-alpha)	2.43	60.52/5.9	58.0/6.1	14	34	↑	13
NP_055317	PRP19	Nuclear matrix protein NMP200 related to splicing factor PRP19	1.69	55.62/6.1	54.3/6.6	12	29	↑	17
NP_004125	HSPA9B	Heat shock 70kDa protein 9B (mortlin-2)	2.43	73.95/5.9	65.8/6.2	22	81	↑	18
NP_006810	STIP1	Stress-induced phosphoprotein1 (Hsp70/Hsp90 -organizing protein)	1.85	63.25/6.4	62.5/6.7	11	26	↑	21
NP_001753	CCT6A	Chaperonin Containing TCP1 subunit 6A	2.43	58.46/6.2	58.5/6.7	21	44	↑	25
AAF13605	HSPA5	BiP Protein	2.43	71.03/5.2	77.5/5.1	20	35	↑	36
AAA35531	PPP2R1A	Medium tumor antigen-associated	2.43	66.06/5.0	60.2/5.2	5	29	↑	37
AAA75240	DMPK	Myotonin-protein kinase, Form II, III, IV	2.43	59.82/4.9	58.4/5.2	9	19	↑	38
CAA04937	SERPINB13	Hurpin	1.68	44.22/5.5	41.7/4.9	6	29	↑	41
NP_009194	COPE	Epsilon subunit of coatomer protein complex isoform a	1.95	34.69/5.0	30.8/5.2	8	24	↑	60
AAH12292	HSPB1	Heat shock 27kDa protein 1	2.43	22.81/6.0	25.7/5.8	14	36	↑	69
AAB58732	PSMD11	26S proteasome subunit 9	2.43	47.66/6.1	45.2/6.5	18	32	↓	32
Q9UQ80	PA2G4	Proliferation-associated protein 2G4	2.43	44.11/6.1	46.3/6.6	11	28	↑	33
Ribonucleoprotein									
AAH03394	HNRPC	Heterogeneous nuclear Ribonucleoprotein C (C1/C2)	2.43	32.38/4.9	37.0/5.1	26	53	↑	45
AAH16736	HNRPF	Heterogeneous nuclear ribonucleoprotein F	2.43	46.02/5.4	45.3/5.5	16	43	↓	55
RNA Binding Protein									
AAL68961	SF4	Splicing factor 4	1.68	72.11/6.9	63.1/6.8	6	21	↑	24
Transcription Factor, Transcription Regulatory Protein									
S45142	DDX48	Translation initiation factor eIF-4A2	2.43	47.10/6.1	47.8/6.6	11	26	↓	31
NP_003745	EIF3S5	Eukaryotic translation initiation factor 3	2.43	37.66/5.2	38.2/5.3	4	26	↓	50
NP_001407	EIF4A1	Eukaryotic translation initiation factor 4A, isoform 1	2.43	46.36/5.3	46.0/5.5	13	32	↓	56
Signal Transduction									
NP_003906	CPNE1	Copine I	2.04	59.67/5.5	61.3/5.8	7	12	↑	12
Energy Metabolism									
NP_001684	ATP6V1B2	ATPase	1.85	56.83/5.6	54.7/5.9	5	13	↑	14
AAA97405	ATIC	AICAR formyltransferase/ IMP	2.43	64.96/6.4	62.0/6.8	11	38	↑	23
NP_006614	PHGDH	Phosphoglycerate dehydrogenase	2.43	57.37/6.3	55.2/6.8	12	22	↑	26
P12268	IMPDH2	Ionosine-5-monophosphate dehydrogenase 2	2.43	56.24/6.4	54.8/6.9	8	16	↑	27
NP_000393	G6PD	Glucose-6-phosphate dehydrogenase	2.43	59.70/6.3	54.7/6.8	23	43	↑	28
AAA51681	AHCY	S-adenosylhomoc-cysteine hydrolase	1.74	48.27/6.0	45.0/6.4	8	39	↓	30
AAA52388	ENO2	Gamma enolase	2.43	44.58/4.9	46.2/5.1	8	24	↑	40
Cellular Organization									
NP_116116	INA	Internexin neuronal intermediate filament protein, alpha	2.43	55.54/ 5.3	57.3/5.7	13	25	↑	7
NP_002264	KRT8	Cytokeratin 8	2.21	53.69/5.5	51.9/5.7	11	20	↑	9
P05787	KRT8	Human Type II cytoskeletal 8	2.42	53.66/5.5	51.6/5.9	9	27	↑	10
NP_005563	LAMNA	Lamin A/C isoform 2	2.43	65.17/6.4	63.6/6.6	20	30	↑	20
AAH00201	WDR1	WDrepeat-containing protein 1	2.43	66.85/6.2	64.3/6.8	9	25	↑	22
NP_005713	ACTR2	Actin-related protein 2	2.43	45.03/6.3	47.7/6.3	10	29	↑	34
BAA08078	CGI1	GDP dissociation inhibitor 1	2.43	51.03/5.2	56.7/5.2	7	14	↑	39
CAA31377	KRT18	Cytokeratin 18	2.43	47.32/5.3	45.3/5.4	15	31	↓	57
NP_004300	ARHGDI A	Rho GDPdissociation inhibitor (GDI) alpha	2.43	23.25/5.0	23.1/5.3	8	36	↑	63
Ionic Channel Protein									
NP_055870	SWAP70	SWAP-70 protein	2.43	69.38/5.6	63.5/6.6	7	12	↑	19
CAB99356	F13A1	Coagulation factor XIII A chain precursor (F13A)	1.85	37.30/5.3	42.3/5.5	4	28	↓	48
NP_001145	ANXA5	Annexin 5	2.43	35.98/4.9	30.0/5.1	16	55	↑	58
AAC25675	CLIC1	Chloride intracellular channel 1	2.43	27.25/5.0	29.0/5.4	8	46	↑	83
NP_001276	CLCA1	Chloride channel	2.43	27.25/5.1	26.5/5.0	5	29	↑	85
Platelet-Derived and Vascular Endothelial Growth Factors (PDGF, VEGF)									
NP_057289	PDGFC	Fallotein	2.43	39.87/5.8	40.2/5.6	4	12	↑	49

^a HUGO, Human genome organization ^b ProFound-peptide Mapping based probability score

Several cytoskeletal or cellular organizational proteins were also 4-PBA-sensitive (Table 1). Most of these proteins fall in the pH range 5–7 and have molecular masses of approximately 45–65 kDa (spot nos. 7, 9, 10, 20, 22, 34, 39, 57, and 63; Figure 4b,c,d,e,g,h). The intensity of six spots was significantly greater in 4-PBA-treated IB3–1 cells than the intensities of those derived from untreated cells. KRT18, a cytosolic network protein that associates with HSP70³⁵ and Δ F508 CFTR,³⁶ was down regulated, whereas KRT8 was up-regulated (spot nos. 9 and 57; Figure 4b,g). Actin-related protein 2 (ACTR2) was up-regulated (spot no. 34; Figure 4d). The ACTR2 protein in association with microtubules is known to promote the transport of misfolded Δ F508-CFTR toward the aggresomes in the ER lumen.³⁷ The up-regulated protein, WD repeat-containing protein 1 (spot no. 22; Figure 4c), is involved in protein–protein interactions and helps to induce the disassembly of actin filaments.^{38,39} Two proteins from the G Protein functional category that are involved in cellular transport and/or endocytosis,^{40,41} were upregulated (spot nos. 39 and 63; Figure 4e and h) by 4-PBA treatment.

A number of ion channels interact physically or in parallel with cAMP-dependent CFTR Cl⁻ channels and amiloride-sensitive ENaC Na⁺ channels. 4-PBA treatment in IB3-1 cells increased two other chloride channel proteins: i. Chloride intracellular channel 1 (CLIC1; spot no. 83; Figure 4h), a member of the p64 family, that exhibits both nuclear and plasma membrane chloride ion channel activity⁴²; ii. Chloride channel, calcium activated protein (CLCA1; spot no. 85; Figure 4h). In addition, three more calcium ion binding proteins, Copine I (spot no. 12; Figure 4b), SWAP-70 (spot no. 19; Figure 4c), and Annexin 5 (spot no. 59; Figure 4h) were found up-regulated by 4-PBA treatment in IB3-1 cells (Table 1). Global up-regulation of cell surface chloride channels in airway epithelia is likely to cause a favorable therapeutic response in CF.

Many metabolic enzymes such as ATPase, AICAR formyl-transferase/IMP, Phosphoglycerate dehydrogenase, Ionosine-5'-monophosphate dehydrogenase 2, Glucose –6-phosphate dehydrogenase and Gamma enolase (spot nos. 14, 23, 26, 27, 28, and 40, Figure 4b,c, and f) were found to be upregulated by 4-PBA treatment of IB3-1 cells indicating an overall positive impact of 4-PBA treatment on metabolic machinery. One exception is S-adenosylhomocysteine hydrolase which was down regulated (spot no. 30, Figure 4d).

Classification of 4-PBA Sensitive Proteins. The identified proteins were further categorized with regard to subcellular localization using the annotations in the Swiss-Prot database (Figure 5). A majority of differentially regulated proteins (~51%) were cytosolic. Other major classes of the identified spots include nuclear proteins 29% followed by endoplasmic reticulum proteins 9% (Figure 5). Fewer proteins were from nuclear membrane (5%), mitochondrial (3%) and plasma membrane (3%).

Western Blot Validation of 4-PBA Modulated Proteins. To further confirm the mass spectrometric identification of key proteins, quantitative immunoblot analysis was used (Figure 6). We selected chaperones which are known to play a central role in protein trafficking and degradation, and verified differential expression by immunoblot analysis. HSP70, GRP78, HOP, TCP1, ACTR2 were up-regulated by 4-PBA (Figure 6 A), and PSMD11, KRT18, were down-regulated (Figure 6 C).

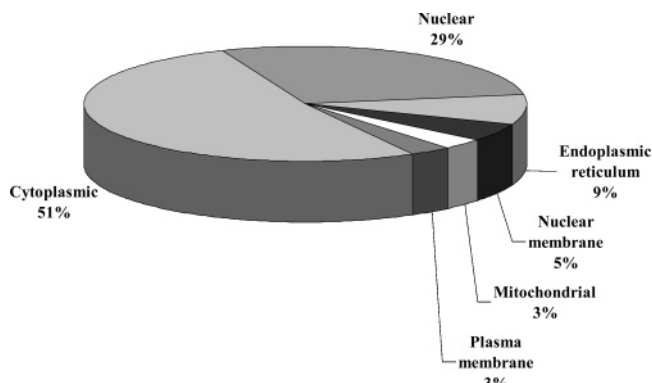


Figure 5. Classification of the identified 4-PBA modulated proteins from IB3-1 cells according to their location. Assignments were made on the basis of information provided on the Swiss-Prot database at the ExpPASy Molecular Biology Server (www.expasy.org).

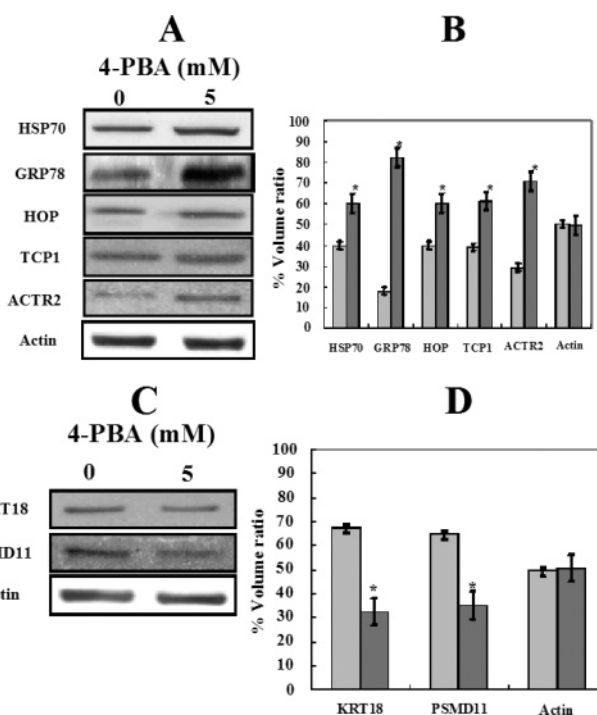


Figure 6. Validation of induction of proteins involved in trafficking and degradation. IB3-1 cells were treated with 5 mM 4-PBA for 48 h and immunoblot analysis was performed as described in the Materials and Methods with 35 μ g total protein lysate in each lane. (A) Proteins upregulated by 4-PBA, HSP70, GRP78, HOP, TCP1, and ACTR2. (B) Densitometric analysis of experiments in (A). (C) Proteins down-regulated by 4-PBA, KRT18 and PSMD11. (D) Densitometric analysis of the experiments in (C). Light bar represents control condition and solid bar represents 4-PBA treatment. Data are the mean \pm SEM of density of gel bands determined from between control ($n = 3$) and 4-PBA treated ($n = 3$) (* $P < 0.05$).

Discussion

The biological response of cells to 4-PBA has been characterized at the mRNA level and with respect to a few of the chaperones.^{20,29–32} Our earlier gene expression profile analysis of 4-PBA treated CF cells suggested that a wide repertoire of genes, including those involved in protein folding, protein transport and ion transport were upregulated, while those

involved in ubiquitin cycle, protein degradation, proteolysis and peptidolysis were downregulated.²⁰ When we compared gene expression profiles at 12 and 24 h of 4-PBA treatment, the strongest effects on mRNA levels were observed at 24 h. On the basis of the wide variation in time course for the translation of changes in mRNA levels to newly equilibrated protein levels, and a preliminary 2-DE analysis of the proteins detected at 1 or 5 mM 4-PBA, we therefore selected 5 mM 4-PBA for 48 h to obtain a comprehensive list of 4-PBA sensitive proteins.

Proteomics refers to the study of the proteome, which is the entire protein complement to a genome. Such global protein expression profiling is advantageous compared with individual gene or protein regulation studies since changes in several functional groups are monitored simultaneously. The objective of this study was to explore the 4-PBA responsive proteome profile of CF airway epithelial cell line (IB3-1), to dissect the molecular networks involved in promoting CFTR processing. We therefore focused the present analysis of 4-PBA modulated proteins on biosynthetic, folding, proteasome-mediated degradation and trafficking/endocytic pathways. Although proteins in low abundance were likely missed, it is clear that 4-PBA has multiple targets (primary and secondary) that may shed new light on mechanisms that control the balance of CFTR biogenesis and proteasome-mediated ubiquitination and degradation pathways.

4-PBA Modulates Protein Folding, Transport, and Trafficking Machinery. Trafficking of wild type or Δ F508-CFTR is aided by transient interactions with molecular chaperones and/or heat-shock proteins. Earlier studies have shown that Δ F508-CFTR remains associated with the cellular chaperone HSP70 to a much greater extent than wild-type CFTR^{10,29-31,43} an association that was suggested to direct mutant CFTR to the ubiquitin-dependent degradation pathway.^{29-32,44} Nevertheless, we and others have previously demonstrated that exposure to 4-PBA facilitates exit of Δ F508-CFTR from the ER to plasma membrane by upregulation of HSP70 and down regulation of HSC70.^{10,45,46} HSC70 has been implicated in the ubiquitination of many misfolded proteins, and been well established that the modulation in HSP70/HSC70 by co-chaperones could facilitate rescue of CFTR.^{29-32,47-49}

In addition to the 70 kD heat shock protein family, the 4-PBA responsive proteome includes several other chaperones and co-chaperones (Table 1). The cellular level of GRP78 (BiP Protein) was significantly upregulated by 4-PBA treatment (spot no. 36, Figure 4e; Figure 6A,B). Although, a role of GRP78 in CFTR trafficking has not been appreciated.⁴³ GRP78 is known to be markedly induced under conditions that lead to the accumulation of unfolded proteins during ER-associated degradation.^{50,51} HSP70, which is closely related to GRP78, is a major cytoplasmic chaperone and protects cells against apoptosis through multiple pathways.⁵² Another stress inducible protein, heat shock 27 kDa protein 1 (Spot no 69, Figure 4h), that has been known for cellular defense⁵² was upregulated and validated from an established atlas of the high abundance CF lung epithelial proteome²⁸ (Table 2).

Additional co-chaperones are known to directly assist in the folding of proteins, and are able to sort the polypeptides for mitochondrial targeting or to target them for degradation by the proteasome.^{29,30,32,47} Our results depict significant upregulation of stress-induced-phosphoprotein 1 (HSP70/HSP90-organizing protein) or "Hop" on 2-DE gels (spot no. 21; Figure 4c) and immunoblot analysis (Figure 6 A). Like the other co-chaperone CHIP,⁴⁸ Hop associates with the C-terminus of

HSP70 via a TPR chaperone adaptor.⁵³ Hop has also been shown to assist in chaperone-mediated protein folding machinery.^{54,55} Although, the role of Hop in regard to CFTR trafficking has not been well-defined yet, modulation in expression level of Hop by 4-PBA in our studies provides an additional signature protein in the putative HSP70/CFTR/HSC70- complex. We did not observe a differential expression of the calcium-sensitive proteins calnexin, and calmodulin.

Molecular chaperone TCP1 subunit 6A (CCT6A) and T-complex protein 1 alpha subunit (TCP1) are eukaryotic chaperonins which associate with ribosome-bound translating polypeptides and mediate protein folding in cytosol. These two proteins were upregulated (spot no. 13, 25; Figure 4b, c: Figure 6 A,B) and since most of the CFTR domains are presented to the cytosol early in biogenesis, these two molecules could play a role in processing. Other than stress inducible chaperone family proteins and their co-chaperones, the chaperonins (TCP1/CCT6A) belong to one of the major chaperone systems that share a common function for binding directly to proteins and thus preventing them from aggregation.⁵⁶

The cytoskeletal protein, KRT18 was downregulated by 4-PBA treatment in IB3-1 cells (spot no. 57, Figure 4g). The depletion in KRT18 level was further confirmed by immunoblot analysis (Figure 6 C,D). Knowing that, KRT18 closely associates with HSP70³⁵ and Δ F508-CFTR,³⁶ one may postulate that the reduction in KRT18 expression levels by 4-PBA may enable Δ F508-CFTR to escape from the ER and reach the plasma membrane, as first suggested by Davezac et al.³⁶ In addition, another filament partner of KRT18, KRT8 was found upregulated after 4-PBA treatment (spot no. 9, Figure 4b). The overexpression of KRT8 in mice has been associated with exocrine pancreatic inflammation,⁵⁷ but CF patients briefly exposed to 4-PBA (7 days) had no evidence of increased pancreatic or systemic inflammation.^{19, 58}

4-PBA Modulates ER-Associated Degradation (ERAD) Proteins. The cytosolic ubiquitin-proteasome pathway plays a key role in ER associated degradation for misfolded CFTR. Upregulation of actin-related protein 2 (ACTR2) by 4-PBA is puzzling (spot no. 34, Figure 4d; Figure 6 A,B), since ACTR2 has been involved in the aggregation of misfolded proteins.³⁷ However, actin filaments can be disassembled by another 4-PBA upregulated molecule WD repeat-containing protein 1 (spot no. 22, Figure 4c). The misfolded protein which has been aggregated with ACTR2 and isolated from the cytoskeleton by WD repeat containing protein 1, can possibly be modified by covalent addition of multiple ubiquitin moieties through the action of cytosolic ubiquitin activating (E1), conjugating (E2), and ligating (E3) enzymes.⁶ These polyubiquitinated polypeptides are then recognized by 26S proteasome subunit 9 (PSMD11) and efficiently degraded.

The 26S proteasome has a central role in the proteolysis of ubiquitinated cellular proteins and is also responsible for cleaving many regulatory proteins such as cyclins, members of the NF- κ B inflammatory signaling family and various other oncogenic products.⁵⁹ The downregulation of 26S subunit 9 (PSMD11) of the proteasome complex may be a common mechanism by which 4-PBA facilitates processing of the Δ F508-CFTR to the trafficking pathway, and decreases degradation of the NF- κ B inhibitor, thereby releasing the IL-8 promoter from NF- κ B mediated induction.

Validation of 4-PBA Modulated CF Proteome with CFTR-Repaired S9 Cells. Pollard et al.²⁸ recently reported a composite atlas of the high abundance CF lung epithelial proteome using

Table 2. Validated Differentially Expressed Protein Spots Regulated by 4-PBA Treatment in IB3-1 Cells with Existing Atlas of CFTR-repaired IB3-1/S9

4-PBA modulated proteins in IB3-1 cells										Pollard et al., 2005 ²⁸					
Locus Link ID	protein description	theor. M_r (kDa)/pI	exper. M_r (kDa)/pI	matches (n)	coverage (%)	spot region/ PBA regulation		accession no.	protein description	theor. M_r (kDa)/pI	exper. M_r (kDa)/pI	matches (n)	coverage (%)	ID no.	map
						Up: (U)	Down: (D)								
Cellular Communication and Signal Transduction															
Protein synthesis, Processing and protein fate															
P17987	TCP-1-alpha	60.52/5.9	58.0/6.1	14	34	b/U		P17987	TCP-1-alpha	60/5.8	NA ^a	7	14	142	2
NP_055317	Nuclear matrix protein NMP200 related to splicing factor PRP19	55.62/6.1	54.3/6.6	12	29	c/U		7657381	Nuclear matrix protein NMP200	55/6.1	NA	13	37	178	2
NP_004125	Heat shock 70kDa protein 9B (mortlin-2)	73.95/5.9	65.8/6.2	22	81	c/U		P11142	HSP70	71/5.4	NA	13	26	282	3
NP_006810	Stress-induced-phosphoprotein1	63.25/6.4	62.5/6.7	11	26	c/U		P31948	STI1 or HOP	63/6.4	NA	41	58	91	2
AAF13605	Bip Protein	71.03/5.2	77.5/5.1	20	35	e/U		NA	NA	NA	NA	NA	NA	NA	NA
AAH12292	HSP 27kDa protein 1	22.81/6.0	25.7/5.8	14	36	h/U		P04792	HSP27	23/6.0	NA	8	38	34	1
AAB58732	26S proteasome subunit 9	47.66/6.1	45.2/6.5	8	20	c/D		NA	NA	NA	NA	NA	NA	NA	NA
AAH03394	Heterogeneous nuclear Ribonucleoprotein C (C1/C2)	32.38/4.9	37.0/5.1	6	23	f/U		P07910	HNRPC	32/5	NA	9	20	133	2
NP_003745.1	Eukaryotic translation initiation factor 3	37.66/5.2	38.2/5.3	4	26	g/D		Q13347	Eukaryotic translation initiation factor 3	37/5.4	NA	6	15	137	2
NP_001407	Eukaryotic translation initiation factor 4A, isoform 1	46.36/5.3	46.0/5.5	13	32	g/D		P04765	Eukaryotic translation initiation factor 4	47/5.3	NA	15	34	58	1
NP_003906.1	Copine I	59.67/5.5	61.3/5.8	7	12	b/U		Q99829	Copine 1	59/5.5	NA	10	15	141	2
NP_000393	Glucose-6-phosphate dehydrogenase	59.70/6.3	54.7/6.8	23	43	c/U		P11413	Glucose-6-phosphate 1-dehydrogenase	59/6.4	NA	15	29	175	2
NP_002264	Cytokeratin 8	53.69/5.5	51.9/5.7	11	20	b/U		P05787	KRT8	54/5.5	NA	20	37	140	2
P05787	Human Type II cytoskeletal 8	53.66/5.5	51.6/5.9	9	27	b/U		P05787	KRT8	54/5.5	NA	15	29	28	1
NP_005713	Actin-related protein 2	45.03/6.3	47.7/6.3	10	29	d/U		NA	NA	NA	NA	NA	NA	NA	NA
CAA31377	Cytokeratin 18	47.32/5.3	45.3/5.4	15	31	g/D		P05783	KRT18	47/5.3	NA	21	33	58	1
NP_004300	Rho GDPdissociation inhibitor (GDI) alpha	23.25/5.0	23.1/5.3	8	36	h/U		NA	NA	NA	NA	NA	NA	NA	NA
NP_001145	Annexin 5	35.98/4.9	30.0/5.1	16	55	h/U		P08758	Annexin V	36/4.9	NA	23	67	29	1
AAC25675	Chloride intracellular channel 1	27.25/5.0	29.0/5.4	8	46	h/U		O00299	Chloride intracellular channel protein 1	27/5.1	NA	5	27	65	1

^aNA: Not available

the CFTR-repaired IB3-1 cells termed S9, which was established by stable infection with an adeno-associated viral vector carrying full length wild-type CFTR.⁶⁰ Comparison of proteins modulated by 4-PBA treatment of IB3-1 cells with the S9 atlas demonstrated that several proteins including TCP1 α , HSP70, HOP, HSP27, Copine 1, KRT8, KRT18, intracellular chloride channel 1, and many others (Table 2) but not the BiP and actin related protein 2, were present in the existing atlas.²⁸ Most of the downregulated proteins from our studies could not be detected in the S9 atlas including 26S proteasomal subunit 9 (PSMD11). We hypothesize that 4-PBA downregulated proteins are not detectable in S9 cells because AAV correction decreases the expression of these proteins below the level of detection.

4-PBA as A Model Drug for CF Therapy. By combining the results of our genomic²⁰ and this proteomic based assessment of 4-PBA on CF cells, new therapeutic targets emerge. Simple rescue of Δ F508-CFTR is unlikely to provide long term therapeutic benefit because the channel is only partially functional and physically unstable, and it is difficult to maintain sufficient levels of CFTR function in the plasma membrane. Therefore, it is desirable to complement the rescue of CFTR with additional interventions. These might include: i. regulation of the actin-based cytoskeletal scaffold to reduce mutant CFTR endocytosis and recycling, ii. upregulation of alternative chloride channels to promote more favorable levels of chloride secretion and to down regulate ENaC, iii. downregulation of the proteasome machinery to reduce the signaling via NF- κ B, and iv. promotion of a favorable metabolic energy balance to sustain epithelial cell activity.

Conclusions

In summary, we have described the first reference map of a pharmacoproteomics approach to study the response to 4-PBA in cystic fibrosis bronchial epithelial cells. The identified proteins fall into several categories and represent a preliminary functional profile of the cystic fibrosis proteome. The 2-DE gel profiles were highly reproducible which is essential for further development of the cystic fibrosis pharmacoproteome database. In addition, we have identified a number of potential stress-responsive candidate proteins that were also identified by other independent methodologies in CF airway epithelial cell lines (IB3-1). This first draft of the CF pharmacoproteome will serve as a basis for further studies of cystic fibrosis proteomics aimed at the identification of potential signature proteins and toward the understanding of mechanisms involved in CFTR biogenesis.

Abbreviations. CFTR, cystic fibrosis transmembrane conductance regulator; CF, cystic fibrosis; 4-PBA, sodium 4-Phenylbutyrate; ERAD, endoplasmic reticulum-associated degradation; MALDI-TOF, matrix-assisted laser desorption ionization time-of flight.

Acknowledgment. This research was supported by R01 HL 59410 and N01 BAA HL 02-04. The authors thank Dr. Robert N. Cole, Director, JHU Proteomics Core Facility. A licensing agreement exists between The Johns Hopkins University, Ucylyed Pharma, Inc., and Dr. Zeitlin. The terms of this arrangement are being managed by the Johns Hopkins University in accordance with its conflict of interest policies. IB3-1 cells are under a licensing agreement between Pfizer Inc., Japan Tobacco Inc. and The Johns Hopkins University. Dr. Zeitlin is entitled to a fee received by the University on sales of this cell

line. The terms of this arrangement are being managed by the Johns Hopkins University in accordance with its conflict of interest policies.

References

- (1) Kerem, B.; Rommens, J. M.; Buchanan, J. A.; Markiewicz, D.; Cox, T. K.; Chakravarti, A.; Buchwald, M.; Tsui, L. C. *Science* **1989**, *245* (4922), 1073–1080.
- (2) Anderson, M. P.; Gregory, R. J.; Thompson, S.; Souza, D. W.; Paul, S.; Mulligan, R. C.; Smith, A. E.; Welsh, M. J. *Science* **1991**, *253* (5016), 202–205.
- (3) Kerem, E.; Corey, M.; Kerem, B. S.; Rommens, J.; Markiewicz, D.; Levison, H.; Tsui, L. C.; Durie, P. N. *Engl. J. Med.* **1990**, *323* (22), 1517–1522.
- (4) <http://www.genet.sickkids.on.ca/cftr/>
- (5) Ward, C. L.; Omura, S.; Kopito, R. R. *Cell* **1995**, *83* (1), 121–127.
- (6) Skach, W. R. *Kidney Int.* **2000**, *57* (3), 825–831.
- (7) Dalemans, W.; Barbry, P.; Champigny, G.; Jallat, S.; Dott, K.; Dreyer, D.; Crystal, R. G.; Pavirani, A.; Lecocq, J. P.; Lazdunski, M. *Nature* **1991**, *354* (6354), 526–528.
- (8) Guggino, W. B.; Banks-Schlegel, S. P. *Am. J. Respir. Crit. Care Med.* **2004**, *170* (7), 815–820.
- (9) Sato, S.; Ward, C. L.; Krouse, M. E.; Wine, J. J.; Kopito, R. R. *J. Biol. Chem.* **1996**, *271* (2), 635–638.
- (10) Choo-Kang, L. R.; Zeitlin, P. L. *Am. J. Physiol. Lung Cell. Mol. Physiol.* **2001**, *281* (1), L58–68.
- (11) Berstrand, C. A.; Frizzell, R. A. *Am. J. Physiol. Cell Physiol.* **2003**, *285* (1), C1–18.
- (12) Arispe, N.; Ma, J.; Jacobson, K. A.; Pollard, H. B. *J. Biol. Chem.* **1998**, *273* (10), 5727–5734.
- (13) Rubenstein, R. C.; Zeitlin, P. L. *Am. J. Physiol. Cell Physiol.* **2000**, *278* (2), C259–267.
- (14) Rubenstein, R. C.; Egan, M. E.; Zeitlin, P. L. *J. Clin. Invest.* **1997**, *100* (10), 2457–2465.
- (15) Monneret, C. *Eur. J. Med. Chem.* **2005**, *40* (1), 1–13.
- (16) Archer, S. Y.; Meng, S.; Shei, A.; Hodin, R. A. *Proc. Natl. Acad. Sci. U.S.A.* **1998**, *95* (12), 6791–6796.
- (17) Crew, T. E.; Elder, D. J.; Paraskeva, C. *Carcinogenesis* **2000**, *21* (1), 69–77.
- (18) Serpe, L.; Laurora, S.; Pizzimenti, S.; Ugazio, E.; Ponti R.; Canaparo R.; Briatore, F.; Barrera, G.; Gasco, M. R.; Bernengo, M. G.; Eandi, M.; Zara, G. P. *Anticancer Drugs* **2004**, *15* (5), 525–536.
- (19) Rubenstein, R. C.; Zeitlin, P. L. *Am. J. Respir. Crit. Care Med.* **1998**, *157* (2), 484–490.
- (20) Wright, J. M.; Zeitlin, P. L.; Cebotaru, L.; Guggino, S. E.; Guggino, W. B. *Physiol. Genomics* **2004**, *16* (2), 204–211.
- (21) Schaub, M.; Keller, W. *Biochimie* **2002**, *84* (8), 791–803.
- (22) Zeitlin, P. L.; Lu, L.; Rhim, J.; Cutting, G.; Stetten, G.; Kieffer, K. A.; Craig, R.; Guggino, W. B. *Am. J. Respir. Cell. Mol. Biol.* **1991**, *4* (4), 313–319.
- (23) Seow, T. K.; Ong, S. E.; Liang, R. C.; Ren, E. C.; Chan, L.; Ou, K.; Chung, M. C. *Electrophoresis* **2000**, *21* (9), 1787–1813.
- (24) Berndt, P.; Hobohm, U.; Langen, H. *Electrophoresis* **1999**, *20* (18), 3521–3526.
- (25) Crawford, I.; Maloney, P. C.; Zeitlin, P. L.; Guggino, W. B.; Hyde, S. C.; Turley, H.; Gatter, K. C.; Harris, A.; Higgins, C. F. *Proc. Natl. Acad. Sci. U.S.A.* **1991**, *88*, 9262–9266.
- (26) Hamosh, A.; Trapnell, B. C.; Zeitlin, P. L.; Montrose-Rafizadeh, C.; Rosenstein, B. J.; Crystal, R. G.; Cutting, G. R. *J. Clin. Invest.* **1991**, *88* (6), 1880–1885.
- (27) Hamosh, A.; Rosenstein, B. J.; Cutting, G. R. *Hum. Mol. Genet.* **1992**, *1* (7), 542–544.
- (28) Pollard, H. B.; Ji, X. D.; Jozwik, C.; Jacobowitz, D. M. *Proteomics* **2005**, *5* (8), 2210–2226.
- (29) Meacham, G. C.; Patterson, C.; Zhang, W.; Younger, J. M.; Cyr, D. M. *Nat. Cell Biol.* **2001**, *3* (1), 100–105.
- (30) Farinha, C. M.; Nogueira, P.; Mendes, F.; Penque, D.; Amaral, M. D. *Biochem. J.* **2002**, *366* (Pt 3), 797–806.
- (31) Younger, J. M.; Ren, H. Y.; Chen, L.; Fan, C. Y.; Fields, A.; Patterson, C.; Cyr, D. M. *J. Cell Biol.* **2004**, *167* (6), 1075–1085.
- (32) Farinha, C. M.; Amaral, M. D. *Mol Cell Biol.* **2005**, *25* (12), 5242–5252.
- (33) Odunuga, O. O.; Longshaw, V. M.; Blatch, G. L. *Bioessays* **2004**, *26* (10), 1058–1068.
- (34) Longshaw, V. M.; Chapple, J. P.; Balda, M. S.; Cheetham, M. E.; Blatch, G. L. *J. Cell Sci.* **2004**, *117* (Pt 5), 701–710.
- (35) Liao, J.; Lowthert, L. A.; Ghori, N.; Omary, M. B. *J. Biol. Chem.* **1995**, *270* (2), 915–922.

- (36) Davezac, N.; Tondelier, D.; Lipecka, J.; Fanen, P.; Demaugre, F.; Debski, J.; Dadlez, M.; Schrattenholz, A.; Cahill, M. A.; Edelman, A. *Proteomics* **2004**, *4* (12), 3833–3844.
- (37) Johnston, J. A.; Illing, M. E.; Kopito, R. R. *Cell Motil. Cytoskeleton* **2002**, *53* (1), 26–38.
- (38) Adler, H. J.; Winnicki, R. S.; Gong, T. W.; Lomax, M. I. *Genomics* **1999**, *56* (1), 59–69.
- (39) Fujibuchi, T.; Abe, Y.; Takeuchi, T.; Imai, Y.; Kamei, Y.; Murase, R.; Ueda, N.; Shigemoto, K.; Yamamoto, H.; Kito, K. *Biochem. Biophys. Res. Commun.* **2005**, *327* (1), 268–275.
- (40) Dovas, A.; Couchman, J. R. *Biochem. J.* **2005**, *390*, 1–9.
- (41) Symons, M.; Rusk, N. *Curr. Biol.* **2003**, *13* (10), R409–418.
- (42) Ashley, R. H. *Mol. Membr. Biol.* **2003**, *20* (1), 1–11.
- (43) Yang, Y.; Janich, S.; Cohn, J. A.; Wilson, J. M. *Proc. Natl. Acad. Sci. U.S.A.* **1993**, *90* (20), 9480–9484.
- (44) Zhang, Y.; Nijbroek, G.; Sullivan, M. L.; McCracken, A. A.; Watkins, S. C.; Michaelis, S.; Brodsky, J. L. *Mol. Biol. Cell.* **2001**, *12* (5), 1303–1314.
- (45) Andersson, C.; Roomans, G. M. *Eur. Respir. J.* **2000**, *15* (5), 937–941.
- (46) Rubenstein, R. C.; Lyons, B. M. *Am. J. Physiol. Lung Cell Mol. Physiol.* **2001**, *281* (1), L43–51.
- (47) Hohfeld, J.; Cyr, D. M.; Patterson, C. *EMBO Rep.* **2001**, *2* (10), 885–890.
- (48) Connell, P.; Ballinger, C. A.; Jiang, J.; Wu, Y.; Thompson, L. J.; Hohfeld, J.; Patterson, C. *Nat. Cell Biol.* **2001**, *3* (1), 93–96.
- (49) Alberti, S.; Bohse, K.; Arndt, V.; Schmitz, A.; Hohfeld, J. *Mol. Biol. Cell.* **2004**, *15* (9), 4003–4010.
- (50) Lee, A. S. *Trends Biochem. Sci.* **2001**, *26* (8), 504–510.
- (51) Ellgaard, L.; Helenius, A. *Nat. Rev. Mol. Cell Biol.* **2003**, *4* (3), 181–191.
- (52) Garrido, C.; Schmitt, E.; Cande, C.; Vahsen, N.; Parcellier, A.; Kroemer, G. *Cell Cycle* **2003**, *2* (6), 579–584.
- (53) Demand, J.; Lüders, J.; Höhfeld, J. *Mol. Cell. Biol.* **1998**, *18* (4), 2023–2028.
- (54) Buchner, J. *Trends Biochem. Sci.* **1999**, *24* (4), 136–141.
- (55) Caplan, A. J. *Trends Cell Biol.* **1999**, *9* (7), 262–268.
- (56) Dunn, A. Y.; Melville, M. W.; Frydman, J. *J. Struct. Biol.* **2001**, *135* (2), 176–184.
- (57) Casanova, M. L.; Bravo, A.; Ramirez, A.; Morreale, de. E. G.; Were, F.; Merlino, G.; Vidal, M.; Jorcano, J. L. *J. Clin. Invest.* **1999**, *103* (11), 1587–1595.
- (58) Zeitlin, P. L.; Diener-West, M.; Rubenstein, R. C.; Boyle, M. P.; Lee, C. K.; Brass-Ernst, L. *Mol. Ther.* **2002**, *6* (1), 119–126.
- (59) Glickman, M. H.; Ciechanover, A. *Physiol. Rev.* **2002**, *82* (2), 373–428.
- (60) Flotte, T. R.; Afione, S. A.; Solow, R.; Drumm, M. L.; Markakis, D.; Guggino, W. B.; Zeitlin, P. L.; Carter, B. J. *J. Biol. Chem.* **1993**, *268* (5), 3781–3790.

PR0503190